Chapter 6

Anodic Aluminum Oxide Template Assisted Chemical Vapor Deposition of Carbon Nanotubes from Acetylene

Abstract

Chemical vapor deposition (CVD) of CNT (length = 55 μm, diameter = 250 - 380 nm, wall thickness = 21 - 100 nm) inside the channels of anodic aluminum oxide (AAO) membranes was carried out at 773 - 1073 K and 1 atm using acetylene (C_2H_2) as the source of carbon. Free-standing CNT arrays were isolated after the AAO membrane was removed by an HF solution. From Arrhenius plot, the energy of activation of the surface-reaction-controlled kinetics is estimated to the 80 kJ mol^{-1}.

6.1 Introduction

There have been many reports about anodic aluminum oxide (AAO) membrane template-assisted growth of CNT from hydrocarbons by chemical vapor deposition (CVD) and related technologies.[1-12,13] By applying different template thickness and pore sizes, the length and diameter of the CNT can be manipulated effectively. A free-standing array of aligned CNT can be fabricated after the removal of the template. However, to our surprise, a thorough study of AAO template assisted CVD of CNT from acetylene (C_2H_2) cannot be found in literature. In addition, most of the reported cases show the need of transition metal catalysts or high energy reaction steps (see Table 6.1).[1-12]

Table 6.1 Summary of AAO assisted CVD of CNT.

Method	Hydrocarbon Source	Flow Rate (sccm)	Temperature (K)	Catalyst	Reaction Time (h)	Wall Thickness (nm)	Ref.
CVD	C_3H_6 (2.5 %) in N_2	200	1073/3073*	—	1	5	2
CVD	C_3H_6 (2.5 %) in N_2	200	1073/3073*	—	1,6,12	3 – 5, 40 – 45, 60 – 80	3
CVD	C_2H_4	10	1173	—	1/6	—	4
CVD	C_3H_6 (2.5 %) in N_2	200	1073	—	1,6,12	3 – 5, 40 – 45, 60 – 80	5
CVD	C_2H_2 (10 %) in N_2	50	973	—	2/3	35	6
CVD	C_2H_4	20	943	—	5.5	40	7
CVD	C_2H_2 (10 %) in N_2	200	973	Co	15	3 – 4	8
CVD	C_2H_2, H_2, N_2 (2%/2%/96%)	100	973 – 1073	Co	1	—	9
CVD	C_2H_2, N_2	—	973	Co	—	—	10
PECVD	C_2H_2 (25%) in N_2	15 – 125	373 – 423 (dc 0 to - 450 V)	—	1/12	—	11
PECVD	C_2H_2, NH_3	—	823	Co	1/4	—	12

* annealing temperature.

Here, we report our investigation and findings on the growth of CNT inside AAO templates from the alkyne. We expect that the technique would allow the design and synthesis of a wide range of CNT with specified geometry and with potential applications in scanning probes, sensors, field emitters, nanoelectronics, and energy storage cells.[14-17]

6.2 Experimental

In a typical reaction, C_2H_2 (San Fu, 99.99%; flow rate: 3 sccm) was supplied to react with a piece of AAO (Whatman Anodisc 13, observed pore average diameter: 280 - 320 nm, thickness: 40 μm) placed in an Ar filled hot-wall atmospheric pressure CVD (APCVCD) reactor at 773 - 1073 K. The AAO substrate turned black after 1 - 3 h. Then, the solid product was removed from the reactor and immersed in an HF solution (48 %) at room temperature. Finally, the solid was washed with boiling D.I. water and dried at 373 K in air.

The samples coated with a thin layer (5 nm) of gold were characterized by scanning electron microscopy (SEM) by using a JEOL JSM-6330F at 15 kV and a HITACHI S-4000 at 25 kV. Transmission electron microscopic (TEM) and high-resolution TEM (HRTEM) images were obtained from a JEOL JEM-2000 FXⅡ at 200 kV and a Philips TECNAI 20 at 200 kV, respectively. Elemental composition of the products was determined by using energy dispersive spectroscopy (EDS; OXFORD Link Pentafet). Fourier transform infrared (FT-IR) spectrum in the range 450 - 4000 cm^{-1} were collected by using a Perkin-Elmer FTIR Spectrum One spectrometer. Laser desorption/ionization mass spectra (LDI-MS) were studied using a Bruker Daltonics Biflex III time-of-flight mass spectrometer equipped with a 337-nm nitrogen laser and a 1.25-m flight tube operated under linear mode. The accelerating voltage was set to 19 kV, while the laser power was carefully adjusted during the analysis to obtain optimized mass resolution. Each mass spectrum was obtained by accumulating 100 laser shots.

6.3 Results and discussion

As summarized in Scheme 6.1, the nanotube arrays were grown from C_2H_2 inside the channels of an AAO membrane at 773 - 1073 K by CVD. Below 773 K, the deposition rate was too low to offer a product. Also, we have observed that the commercial AAO membranes, with a bigger pore sizes of ca. 200 - 300 nm, show better assistance to the nanotube formation than homemade templates with a smaller pore sizes of 60 nm. This is attributed to the easiness of diffusion of the reactant within the pore.

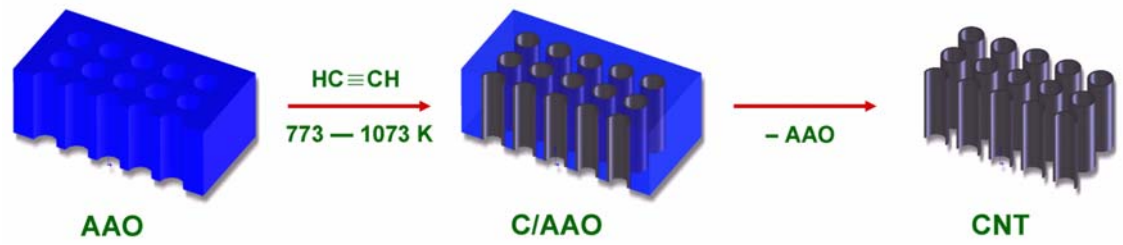

Scheme 6.1 CNT formation process.

In Figure 6.1, optical and SEM photographs of the physical appearance and the microscopic morphology of the as deposited products are shown. It can be seen in the optical images in Figures 6.1 (a) - 6.1 (c) that the AAO templates turned black after the deposition process was completed. As the temperature of deposition was increased, the quantity of acetylene black particles, byproducts from homogeneous gas phase decomposition reactions, accumulated on the quartz boat increased as well. In addition, it can be seen that the membranes curled significantly as the temperature of deposition was increased. This is probably the result of the thermal expansion difference of AAO and the deposited carbon. From the SEM images in Figures 6.1 (d) - 6.1 (f), it is clear that inside the porous channels of the AAO membranes, nanotubes with an average diameter of 250 - 380 nm were grown. The average wall thickness increased from 21 to 100 nm as the temperature of deposition was increased from 773 to 1073 K. Figure 6.1 (d) shows the sample grown at 773 K. The nanotubes are shown to have thin walls. In addition, a few particles can also be found. In Figure 6.1 (e), it is observed that uniform nanotubes grown at 873 K form a hexagonally ordered structure inside the honeycomb shaped AAO channels. Figure 6.1 (f) shows that the nanotubes deposited at 1073 K grew along the channels inside the AAO template. It also shows that, on the lower right corner of the image, the very top surface of the template was filled with more deposited material and the channel openings were drastically narrowed.

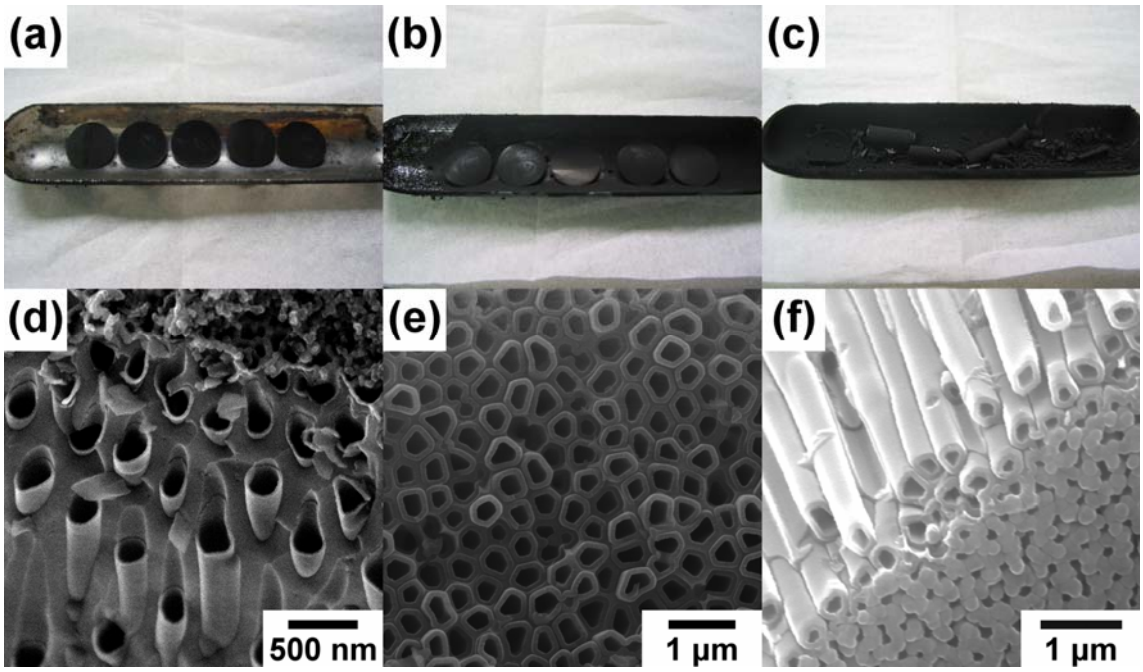

Figure 6.1 Photographs of CNT containing AAO membranes. Deposited at (a) 773, (b) 873, and (c) 1073 K. SEM images of CNT containing AAO membranes. Grown at (d) 773, (e) 873, and (f) 1073 K.

Figure 6.2 displays the electron micrographs of the CNT grown at 773 and 1073 K after the AAO membranes were removed by 48 % HF. From the SEM image in Figure 6.2 (a), the average length of the highly aligned CNT prepared at 773 K is estimated to be 55 μm. This agrees with the AAO template thickness. In Figure 6.2 (b), a representative bright field TEM micrograph of a sample grown at 773 K shows that the tubes have an average diameter of 260 nm and a uniform wall thickness of 21 nm. A diffused ring pattern in the electron diffraction (ED), the inset of Figure 6.2 (b), indicates that the nanotubes are amorphous. This is also supported by the HRTEM image of the wall structure of a CNT in Figure 6.2 (c). In Figure 6.2 (d), the SEM image of an AAO-free CNT bundle grown at 1073 K from C_2H_2 is shown. The average length of the CNT is 40 μm, in good agreement with the template thickness. From the TEM image in Figure 6.2 (e), the average tube diameter and the wall thickness of the CNT is estimated to be 380 nm and 100 nm, respectively. The ED pattern in the inset of

Figure 6.2 (e) shows the reflections corresponding to (002) planes of graphite. The interlayer spacing is estimated to be 0.35 nm, which agrees with the value estimated from the HRTEM image shown in Figure 6.2 (f). The spacing is slightly larger than the literature value of graphite, 0.335nm. Using EDS, the composition of the CNT sample is confirmed to be pure carbon.

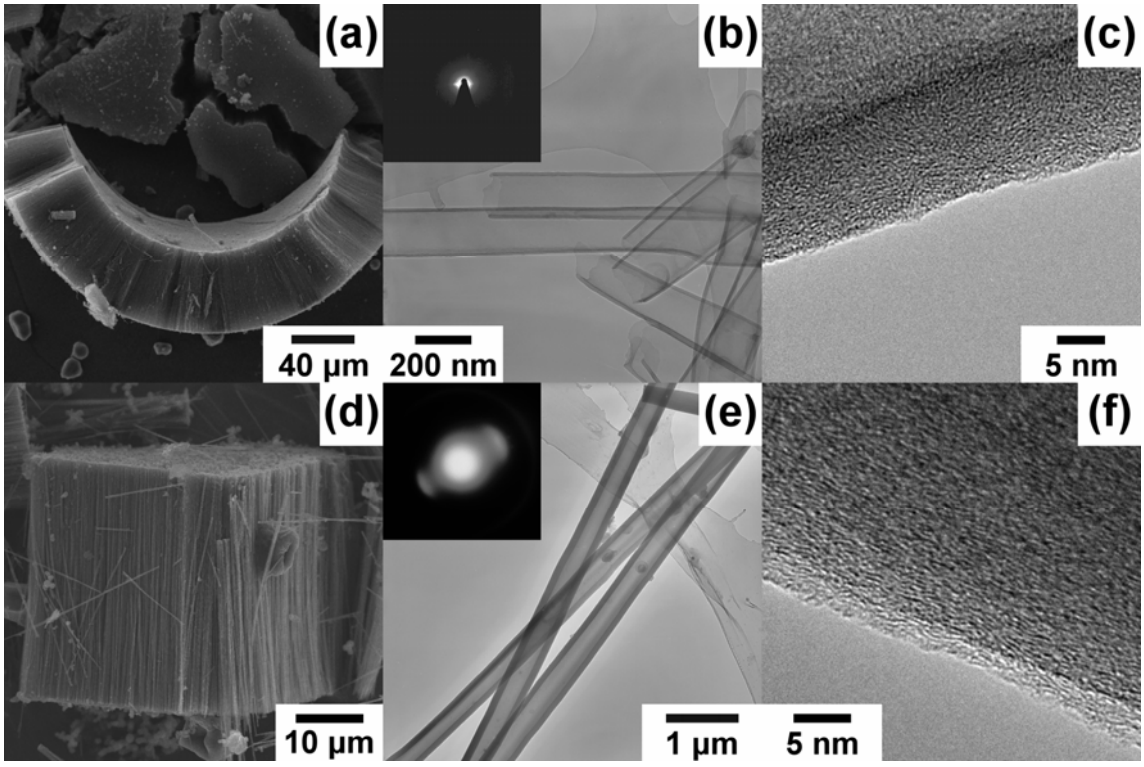

Figure 6.2 Electron micrographs of AAO-free CNT. Grown at 773 K, (a) SEM image of a bundle of CNT, (b) TEM image of some CNT, and (c) HRTEM image of wall structure of CNT shown in (b). Grown at 1073 K, (d) SEM image of a bundle of CNT, (e) TEM image of some CNT, and (f) HRTEM image of wall structure of CNT shown in (e).

In Figure 6.3, a montage of sections of a CNT deposited at 873 K is shown. It is clear that the section in Figure 6.3 (a) is close-ended. More to the right, the image shows thinner CNT walls as shown in Figure 6.3 (e). We speculate that the sections on the left were grown on the top of the AAO while the rest were deposited in the channels.

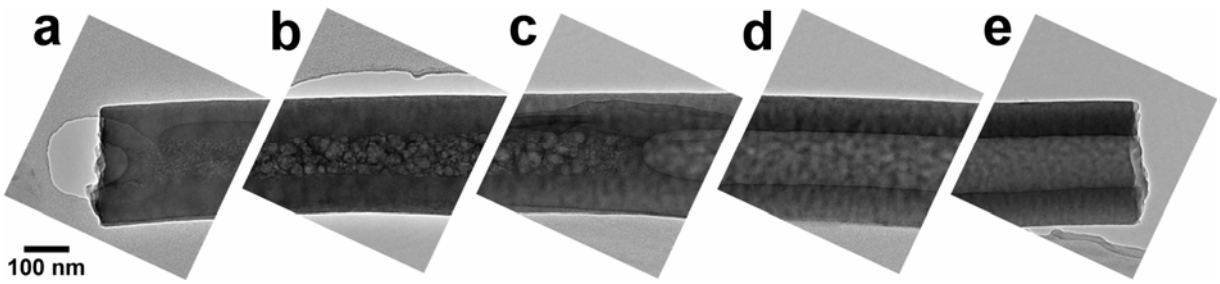

Figure 6.3 Montage of TEM images of an individual CNT grown at 873 K.

In order to understand the growth kinetics, a series of as-deposited samples, grown at 773 - 1273 K, were weighed. The growth rates were calculated and plotted against 1/T, as shown in the Arrhenius plot in Figure 6.4. Two regions, showing distinctive slopes can be seen at 773 - 973 K and 973 - 1273 K. From the slopes, the apparent energies of activation (E_a) of the process can be estimated. The lower temperature region suggests a value of 80 kJ mol^{-1}. This is significantly lower than the HC_2-H bond dissociation energy, 552 kJ mol^{-1} reported in literature.[18] The calculated E_a is typical for a CVD process that is surface catalyzed and surface-reaction-controlled.[13] The higher temperature region shows a nearly flat slop, which suggests that the reaction is diffusion-controlled. It is interesting to note that comparing to many other CVD processes,[19-20] the CNT formed in this study has an extremely high aspect ratio of 220. This has been observed in other cases forming CNT from AAO templates.[2-7] The overall growth steps can be described briefly as follows. AAO has been known to be crystalline γ- Al_2O_3,[21-22] a material with a high dehydrative catalytic activity. Therefore, at the initial stages of the deposition process, C_2H_2 was readily decomposed on the surface in the porous channels of AAO to form carbonaceous deposits, which passivated the AAO surface. As the surface reactivity was decreased on the carbon covered area, C_2H_2 molecules could diffuse inner and decompose deeper into the channels until the whole channels were covered. The overall process of the first layer growth might resemble an atomic layer deposition (ALD) process.[23] Another possible origin for the formation of the high aspect ratio material is that the reactivity of C_2H_2 was very low at the reaction conditions. This might allow more molecules

to diffuse into the AAO channels without decomposition even the mean-free-path is low at the reaction pressure. Since the growth temperature was not high enough, the carbon atoms did not crystallize well in the CNT. As the temperature of deposition was increased, the deposition rate reached a constant, as shown in Figure 6.4. This probably was the consequence that the diffusion of C_2H_2 was limited significantly as the top layer no the AAO surface was gradually sealed off.

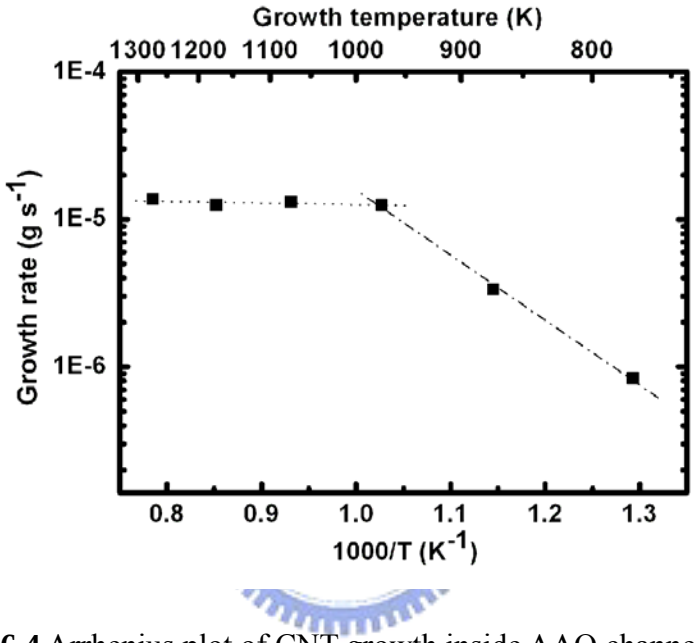

Figure 6.4 Arrhenius plot of CNT growth inside AAO channels from C_2H_2.

The FT-IR spectrum of the sample grown at 773 K, shown in Figure 6.5, indicates the presence of residual C=C, C-C, C-O and C-H vibrations in the range 750 - 1750 cm^{-1}. In addition, a broad O-H stretching and a weak C-H stretching were observed (not shown) at 3250 - 3680 cm^{-1} and at 2920 cm^{-1}, respectively. The spectrum indicates that the deposited carbon material had many defects and yet to be crystallized. This is consistent with the ED study in Figure 6.2 (b). The observed signals decreased as the growth temperature increased from 773 to 1073 K. And the sample graphitized more completely, as shown in Figures 6.2 (e) and 6.2 (f).

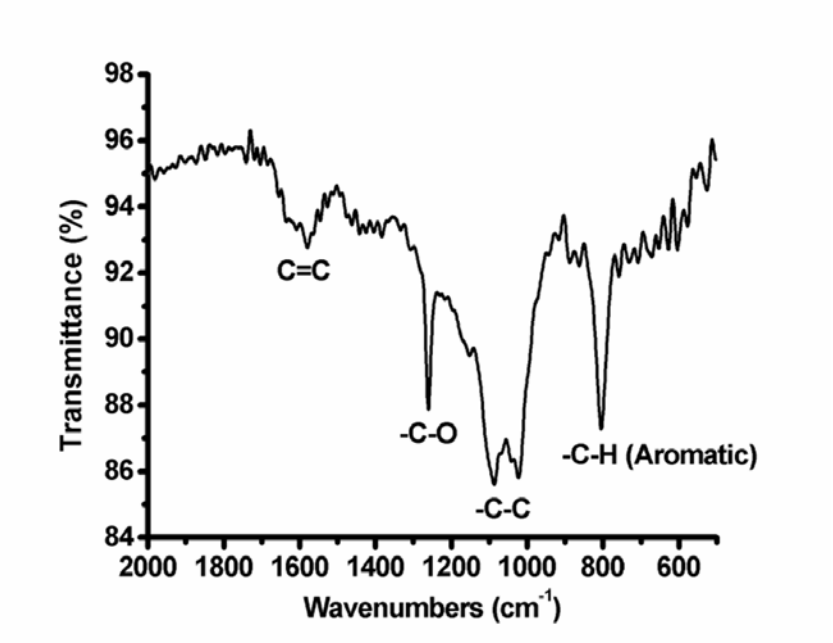

Figure 6.5 FT-IR spectrum of CNT fabricated at 773 K.

The LDI-MS spectra of the samples grown at 773 – 1073 K are shown in Figure 6.6. The desorbed carbon species have a mass value (m/z) span of 1000 – 3500. Maxima of the masses are evenly separated at a spacing of multiples of 24 amu. Apparently, the difference of the species are the loss of $(C_2)_n$ species. This is a well-known feature in the mass spectral pattern of fullerenes and other carbon materials.[24-27]

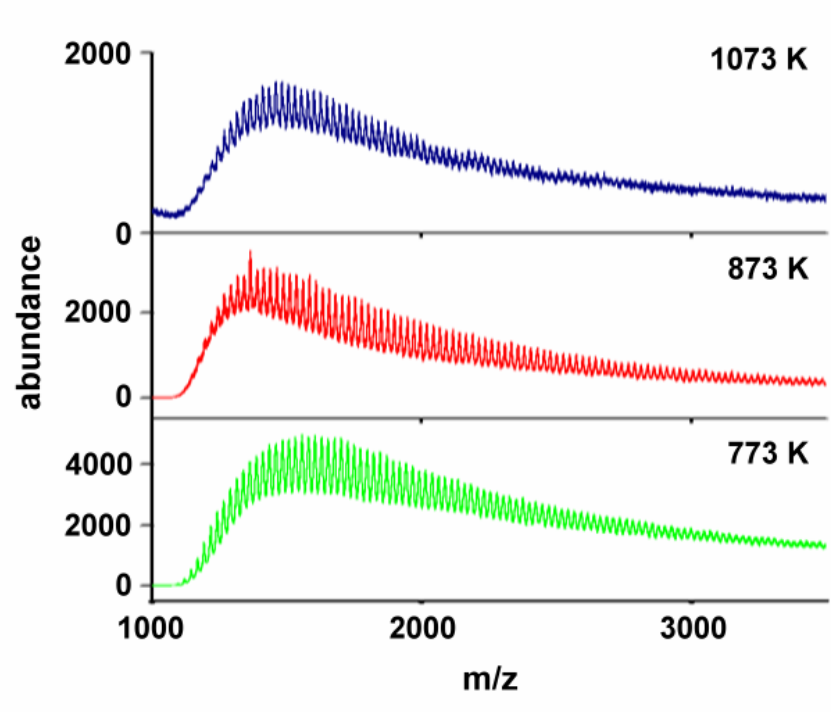

Figure 6.6 LDI-MS spectra of CNT grown at 773 – 1073 K.

6.4 Conclusion

In summary, we have synthesized highly-ordered CNT arrays over a large area on AAO from acetylene by CVD. The growth property of CNT were closely related to the structure of the deposition temperature and time. We found that the pyrolysis temperature of acetylene to deposit carbon atom starts above 773 K. Increasing the temperature of deposition to 1073 K, CNT with more ordered graphite structure can be obtained. The study provides a simple low cost, low temperature, and controllable technique to grow CNT. The highly-oriented and isolated CNT array membranes could be very useful in a variety of applications.

References

1. Huczko, A. *Appl. Phys. A* **2000**, *70*, 365.
2. Kyotani, T.; Tsai, L.-F.; Tomita, A. *Chem. Mater.* **1995**, *7*, 1427.
3. Kyotani, T.; Tsai, L.-F.; Tomita, A. *Chem. Mater.* **1996**, *8*, 2109.
4. Che, G.; Lakshmi, B. B.; Martin, C. R.; Fisher, E. R. *Chem. Mater.* **1998**, *10,* 260.
5. Kyotani, T.; Pradhan, B. K.; Tomita, A.; Kyotani, T.; Pradhan, B. K.; Tomita, A. *Bull. Chem. Soc. Jpn.* **1999**, *72*, 1957.
6. Shelimov, K. B.; Moskovits, M. *Chem. Mater.* **2000**, *12*, 250.
7. Miller, S. A.; Young, V. Y.; Martin, C. R. *J. Am. Chem. Soc.* **2001**, *123*, 12335.
8. Li, J.; Moskovits, M. Haslett, T. L. *Chem. Mater.* **1998**, *10*, 1963.
9. Iwasaki, T.; Motoi, T.; Den, T. *Appl. Phys. Lett.* **1999**, *75*, 2044.
10. Suh, J. S.; Lee, J. S. *Appl. Phys. Lett.* **1999**, *75*, 2047.
11. Shung, S. L.; Tsai, S. H.; Tseng, C. H.; Chiang, F. K.; Liu, X. W.; Shih, H. C. *Appl. Phys. Lett.* **1999**, *74*, 197.
12. Kim, M. J.; Lee, T. Y.; Choi, J. H.; Park, J. B.; Lee, S.; Kim, S. K.; Yoo, J.-B.; Park, C.-Y. *Diamond Relat. Mater.* **2003**, *12*, 870.
13. Chiu, H.-T. *Chemical Vapor Deposition*, http://www3.interscience.wiley.com/cgi-bin/mrwhome/104554789/HOME, *Kirk-Othmer Encyclopedia of Chemical Technology Online Edition*, John Wiley & Sons, 2004.
14. Service, R. F. *Science* **1998**, *281*, 940.
15. Dai, H.; Hafner, J. H.; Rinzler, A. G.; Colbert, D. T.; Smalley, R. E. *Nature* **1996**, *384*, 147.
16. de Heer, W. A.; Châtelain, A.; Ugarte, D. *Science* **1995**, *270*, 1179.
17. Baughman, R. H.; Zakhidov, A. A.; de Heer, W. A. *Science* **2002**, *297*, 787.

18. Ervin, K. M.; Shi, Y. *Bond Dissociation Energies of the Polyynes: $D_0(HC_{2n}–H)$ is smaller than $D_0(HCC–H)$ for n > 2*, http://www.cstl.nist.gov/div838/kinetics2001/agenda/j_session/j8/j8.htm, *5th International Conference on Chemical Kinetics, 16 - 20 July 2001*, National Institute of Standards and Technology: Gaithersburg, Maryland.
19. Tsai, M. H.; Sun, S. C.; Chiu, H. T.; Tsai, C. E.; Chuang, S. H. *Appl. Phys. Lett.* **1995**, *67*, 1128.
20. Tsai, M. H.; Sun, S. C.; Chiu, H. T.; Chuang, S. H. *Appl. Phys. Lett.* **1996**, *68*, 1412.
21. Jeong, S. H.; Hwang, H. Y.; Hwang, S. K.; Lee, K. H. *Carbon* **2004**, *42*, 2073.
22. Morterra, C.; Magnacca, G. *Catal. Today* **1996**, *27*, 497.
23. Hausmann, D.; Becker, J.; Wang, S.; Gordon, R. G. *Science* **2002**, *298*, 402.
24. O'Brien, S. C.; Heath, J. R.; Curl, R. F.; Smally, R. E. *J. Chem. Phys.* **1988**, *88*, 220.
25. Lagow, R. J.; Kampa, J. J.; Wei, H. C.; Battle, S. L.; Genge, J. W.; Laude, D. A.; Harper, C. J.; Bau, R.; Stevens, R. C.; Haw, J. F.; Munson, E. *Science* **1995**, *267*, 362.
26. Ramesh, S.; Brinson, B.; Johnson, M. P.; Gu, Z.; Saini, R. K.; Willis, P.; Marriott, T.; Billus, W. E.; Margrave, J. L.; Hauge, R. H.; Smally, R. E. *J. Phys. Chem. B* **2003**, *107*, 1360.
27. Sadana, A. K.; Liang, F.; Brinson, B.; Arepalli, S.; Farhat, S.; Hauge, R. H.; Smally, R. E.; Billups, W. E. *J. Phys. Chem. B* **2005**, *109*, 4416.